R. & M. No. 3007
(14,892)
A.R.C. Technical Report

MINISTRY OF SUPPLY

AERONAUTICAL RESEARCH COUNCIL
REPORTS AND MEMORANDA

# The Effect of a Spike Protruding in Front of a Bluff Body at Supersonic Speeds

*By*

D. BEASTALL and J. TURNER



LONDON: HER MAJESTY'S STATIONERY OFFICE
1957
EIGHT SHILLINGS NET

# The Effect of a Spike Protruding in Front of a Bluff Body at Supersonic Speeds

*By*

D. BEASTALL and J. TURNER

COMMUNICATED BY THE PRINCIPAL DIRECTOR OF SCIENTIFIC RESEARCH (AIR), MINISTRY OF SUPPLY

*Reports and Memoranda No.* 3007*

*January,* 1952

*Summary.*—Wind-tunnel tests at $M = 1{\cdot}5$, $1{\cdot}6$ and $1{\cdot}8$ are described in which the effect of mounting a stem, with different nose pieces, on the forward face of a bluff-nosed body is studied. The drag on the front face of the body was derived from pressure measurements for different projections of the stem.

Schlieren equipment was used and several interesting phenomena observed in the flow are discussed, in particular a flow oscillation resembling that which sometimes occurs with centre-body intakes.

1. *Introduction.*—It has been found that a reduction in drag could be obtained by mounting on the nose of the body a thin cylindrical rod on the end of which was a small conical body (Fig. 1). The reason given for the reduction in drag was that the conical nose substituted a conical shock in place of the strong detached shock which occurred in front of the bluff body alone ; the flow after the shock then followed a path (shown dotted in Fig. 1) in much the same way as if there was a complete ogive nose there. The more nearly the size of the cone was increased to approach the ogive nose the less the drag became.

In some tests in connection with experiments on flow separation carried out in the Royal Aircraft Establishment $5\frac{1}{2}$ in. $\times$ $5\frac{1}{2}$ in. Supersonic Wind Tunnel it was found that the presence of a thin cylindrical rod, sharpened to a point at the forward end, and fixed on the front of a bluff body (Fig. 2) also reduced the drag. From Schlieren observation it could be seen that the flow attached to the rod for some of its length and then separated, forming a conical shock and a roughly conical dead-water region in front of the body.

The wind-tunnel tests described here were initiated to compare the two methods of reducing the drag and in the course of the tests several interesting flow phenomena were noticed. The tests were designed to study the effect on the drag of changing the length of projecting rod in front of the bluff body and to this end pressures were measured on the front face of the body (a right cylinder) and Schlieren observation was used.

The results, apart from the drag variations shown, give useful data in connection with the operation of centre-body diffusers, the shock oscillation which occurs for certain lengths of rod projection being considered to be similar in character to the large shock oscillation encountered

*R.A.E. Technical Note Aero 2137, received 12th May, 1952.

on certain centre-body diffusers. The results may also lead to a better understanding of the effect of boundary-layer characteristics on flow separation and on the occurrence of an over-expansion bubble at the shoulder of bluff bodies.

2. *Experiment.*—2.1. *Test Programme.*—The previous tests on the reduction of drag of bluff bodies by means of a forward projecting stem, with or without a conical nose piece, had not been systematic and gave little indication of the advantages of one type of projection over another or of the optimum length of projection for least drag. The purpose of the present tests was to examine more closely the flow over bluff bodies with projections for a limited Mach number range. Accordingly the change in the flow pattern caused by changes in the length of stem and size of nose piece were observed by Schlieren for a cylindrical body and stem with different conical attachments. The tests were made at $M = 1{\cdot}5$, $1{\cdot}6$ and $1{\cdot}8$ in the 9 in. $\times$ 9 in. Supersonic Wind Tunnel at the R.A.E. at atmospheric stagnation pressure. The drag on the front face of the cylinder was calculated from pressure measurements as the stem was extended. From the results it was possible to give values of stem projection and cone angle which gave the least drag.

In the course of the Schlieren observation several changes in the flow patterns were noticed which are considered of general interest and these are discussed.

2.2. *Equipment.*—The tests were carried out in the R.A.E. 9 in. $\times$ 9 in. Closed Circuit Supersonic Wind Tunnel at Mach numbers $1{\cdot}5$, $1{\cdot}6$ and $1{\cdot}8$ and a Reynolds number of roughly $0{\cdot}75 \times 10^6$ per inch. The arrangement of the bluff body with the projecting stem and alternative nose pieces is shown in Fig. 3. Control of the projection of the stem was possible from outside the tunnel. The bluff body was a $1\frac{1}{2}$ in. diameter cylinder 3 in. long with the front face plane and normal to the flow. The body was mounted on a sting which also served as a housing for the stem when withdrawn into the body. The stem was a $\frac{1}{4}$ in. diameter rod which could extend a distance of 7 in. in front of the cylindrical body. Cones of length $0{\cdot}65$ in. and semi-angles 15 deg, 30 deg and 40 deg, and an ogive nose were used for attachment to the front of the stem. Three holes spaced radially on the front face of the cylinder at $0{\cdot}25$ in., $0{\cdot}45$ in. and $0{\cdot}65$ in. radii gave pressures from which the drag coefficients were calculated.

3. *Tests and Results.*—3.1. *Pressure Measurements.*—Readings of the pressures on the front face of the bluff body were taken for each $\frac{1}{4}$ in. projection of the stem, up to a maximum projection of 7 in., with all alternative nose pieces. The pressures were taken with the stem extending and receding as there was a hysteresis in the flow changes in most cases. The pressures, given as a proportion of the tunnel stagnation pressure $p_0$, are given in Tables 1 to 12. A plug replaced the stem so that the pressures on the bluff body alone could be measured and these are given in Table 13.

3.2. *Drag Coefficients.*—The drag coefficients were derived from the measured pressures (expressed as differences from the free-stream static pressures) and are plotted in Figs. 4 to 7. The drags include the pressure drags of the alternative nose pieces but do not include skin friction. The pressure drag of a conical nose piece was obtained by assuming the theoretical value on the conical surface and by assessing the pressure on the base of the cone from Schlieren photographs. The drag of the ogive nose piece was estimated roughly by assuming it to be a mean cone of $7\frac{1}{2}$ deg semi-angle. These values of the nose-piece drag were added to the body frontal drag for all stem positions but strictly only apply when the stem projection is such that the nose piece is ahead of the detached shock in front of the body and also out of the range of flow oscillation.

There is a hysteresis in the flow changes, the drag for a certain range of stem projections depending on the direction in which the stem has been moved ; the direction of movement in such cases is denoted by arrows in the Figs. 4 to 7. To provide some basis for assessing the reduction of drag due to the nose pieces, the drag coefficients of equivalent cones over a range

of cone semi-angles, are plotted in each of Figs. 4 to 7. For example it can be seen from Fig. 4 that the drag of the bluff body for a stem extension of 2·58 in. at $M = 1{\cdot}6$ is reduced to that of a 24 deg semi-angle cone of the same frontal area. This value agrees quite well with the angle of separation measured from the corresponding Schlieren photograph (Fig. 15).

3.3. *Schlieren Observation.*—The different types of flow encountered in the tests are best illustrated by Schlieren photographs and as there were no fundamental differences between the flow changes at the different Mach numbers the main points will be illustrated for $M = 1{\cdot}6$ only. The sequence of flow patterns as the stem is pushed forward will be illustrated and discussed. Note that the stem extension is defined as the distance of the tip of the ogive nose piece from the front face of the body but as the distance of the bases of the conical nose pieces from the front face of the body.

The first phase to be dealt with will be the changes in the flow up to the point at which the tip of the nose piece touches the detached shock ahead of the body. Fig. 8 shows the bluff body alone with the over-expansion bubble just aft of the shoulder clearly visible and roughly 0·8 in. long. The length of this bubble is reduced as the stem (with any nose piece) is projected forward as far as the shock. Figs. 9 and 10 illustrate this for the ogive nose. Presumably this is connected with the flow changes over the front face of the body which occur as the stem moves forward. The flow changes are, however, insufficient to change the shape of the detached shock noticeably.

As soon as the nose piece pierces the shock a high-frequency oscillation starts in the case of the ogive and 15 deg semi-angle cone nose pieces but not with the 30 deg and 40 deg semi-angle cones ; the oscillation can be heard as a high pitched whistle. The types of flow for the different nose pieces can be compared from Figs. 11, 12, 13 and 14. In Fig. 11 is shown the Schlieren photograph that results from the unsteady flow that occurs with the ogive nose piece. The blurred image is a result of the shock oscillation. The shock configuration appears to alternate between an ordinary detached shock ahead of the body and a curved shock passing through the point of the nose piece. The ordinary detached shock shows up very light in the lower half of the photograph of Fig. 11 ; its position appears to be slightly closer to the body than the shock for the bluff body alone (Fig. 8). A similar photograph is shown in Fig. 12 for the 15 deg semi-angle nose piece. In this case the rearward detached shock trace appears to be even closer to the body than in Fig. 11.

This oscillation does not occur when the 30 deg and 40 deg semi-angle cones are pushed up to the detached shock. (The Schlieren photographs for these cases are given in Figs. 13 and 14.) Instead, the detached shock sticks to the points of the cones and its shape is modified, as the cone moves forward, from the curved detached shock to the shock shape corresponding to that in front of the cone. The cone apparently pushes the shock into a new shape. What determines whether a conical nose piece in conjunction with a given body will be prone to oscillation is not immediately apparent but it is obvious from observation that the greater the cone angle the less the likelihood of oscillation. A study of the flow pattern over the conical nose pieces in Figs. 13 and 14 reveals that there is a flow separation from the base of the cone which strikes the shoulder of the body and encloses a dead-air space between the cone and body. In both Figs. 13 and 14, this separated flow is inclined at a smaller angle to the axis of the body than the conical surface is. For smaller cone angles, however, this may not be so and in such a case there would be a tendency for the point of separation to move along the conical surface towards the tip of the cone. It is suggested that this in fact happens for the smaller angle cones and consequently the separation interferes with the nose stock, resulting in an oscillatory flow.

Although this main shock oscillation is avoided by the use of larger angle cones there is a small flow oscillation apparent in Fig. 13. The flow separation from the cone and the expansion at the shoulder of the body are indistinct and are actually unsteady. The corresponding parts of the flow in Fig. 14 are well defined and there is no oscillation. The oscillation could be heard as a whistle which changed pitch as the position of the cone was varied but the noise level was

much less than for the main oscillation. Once again the reasons for this oscillation, which is quite apart from the main one, are not obvious but the following explanation is offered. The boundary of the separated flow from the base of the cone which is of a different velocity from the main flow acts in much the same way as a jet of air playing on the knife edge of an organ pipe, a certain length of jet exciting a certain column of air. In this case the length of jet is the length of the mixing zone between the shoulder of the cone and the shoulder of the body, and the column of air is the dead-air space between the cone and body.

Now let us consider what happens when the nose pieces are pushed still further forward. A point is reached at which the main oscillation ceases and the steady flow conditions shown in Figs. 15 and 16 are attained. The stem extension at which the oscillation ceases corresponds to the point in Tables 5 and 6 at which there is a substantial decrease in pressure on the face of the body (roughly 2 in. extension in both cases). There is no appreciable change in flow pattern with the 30 deg and 40 deg semi-angle cones. The small oscillation at the shoulder of the body still persists, however, in most instances as is seen by the blurred images of the flow there. The pitch of the note given out by the oscillation changes however as the stem position is changed.

The flow for the 15 deg semi-angle cone is now similar to that for the larger angle cones (*cf.* Fig. 13, 14 and 16) but the flow pattern over the ogive nose and stem is slightly different. The flow adheres to the ogive after the nose shock and then separates from the stem forming a nearly conical dead-air space ahead of the body.

Now let us consider further extension of the stem ahead of the body. Firstly, there are no further big changes in the flow pattern over the ogive nose piece and body ; the only slight change is that after a certain stem extension the point of flow separation from the stem appears to be more clearly defined than for shorter stem extensions. This may well be when the point of transition of the boundary layer on the stem lies ahead of the point of separation, as the more abrupt separation of Fig. 17 suggests a turbulent layer and the more gradual separation of Fig. 15 a laminar layer. This change in the form of the separation coincides roughly with the point in Fig. 4 at which the pressure/drag coefficient starts to decrease more rapidly (at roughly $4\frac{1}{2}$ in. extension).

The three conical nose pieces show no major flow changes up to a certain point (Figs. 18, 19 and 20). Once this point, which differs for each cone and Mach number, is reached there is an abrupt change in the flow pattern. This new type of flow pattern is shown in Figs. 21 and 22 for the 15 deg and 30 deg semi-angle cones. The change point for the 40 deg semi-angle cone was never reached at $M = 1{\cdot}5$. The change to the new flow pattern takes place as follows. The separation boundary from the shoulder of the cones become flatter and flatter as the stem is pushed out (*cf.* Figs. 13 and 19) and then instead of passing across to the shoulder of the body it attaches to the stem and then separates again in front of the body in much the same way as the flow separates from the stem with the ogive nose piece. The change to this new pattern is abrupt. After this change no further change in the flow configuration takes place with further stem extension.

If now the stem is withdrawn into the body the flow will revert to its original pattern but not at the same stem extension. There is in fact a hysteresis effect which can be seen by comparing Figs. 23 and 24 with Figs. 18 and 19 respectively. The stem extensions of Figs. 23 and 24 are less than the corresponding extensions for Figs. 18 and 19 and yet the flow has not reverted to the original state. This hysteresis can also be seen clearly in the drag coefficients of Figs. 5 to 7 where the drag depends on the direction of motion of the stem. Apart from this one range of hysteresis the rest of the flow patterns are independent of the direction from which the stem has moved.

4. *Discussion of Results.*—The results of the wind-tunnel tests on a bluff body and forward extending stem with various nose pieces comprise (*a*) pressure measurements on the front face of the body (from which the drag coefficients have been derived) and (*b*) Schlieren observation

of the flow, over a range of stem extensions for $M = 1{\cdot}5$, $1{\cdot}6$ and $1{\cdot}8$. The results have been presented in section 3 and related figures and tables, the salient points of which will now be discussed.

4.1. *Bluff Body Drag.*—In Table 13 the pressures on the face of the bluff body alone are compared with the theoretical pressure behind a plane shock (both given as ratios of the stagnation pressure). It is interesting to note that a pitot-tube will experience a greater drag than a sawn off cylindrical body of the same dimensions, which suggests a fundamental difference in the flow over open-ended and closed cylinders.

4.2. *Over-expansion.*—From Figs. 8, 9 and 10 the reduction of the extent of the over-expansion region at the shoulder of the body is apparent as the stem is moved forward. At the same time the pressures on the face of the body (Table 5) are altered slightly. This suggests that the occurrence and extent of a region of over-expansion is dependent upon the pressure prevailing at the shoulder on the front face of the body.

4.3. *Flow Oscillation.*—Two types of flow unsteadiness have been observed, the first, as shown in Figs. 11 and 12, being a violent oscillation and the second, as shown in particular in Fig. 13, being a much milder one. The violent oscillation only occurs with the ogive and 15 deg semi-angle conical nose pieces but the mild oscillation does not seem to depend on the nose piece and may occur for any stem extension where there is a dead-air space between the stem and the body.

The factors which appear to determine whether or not the violent flow oscillation will occur are :

(*a*) the cone angle of the nose piece

(*b*) the position of the nose piece relative to the body

(*c*) the shape and position of the detached shock ahead of the body (this is a function of Mach number and the shape of the body).

To examine how these factors decide whether or not flow oscillation will take place let us consider the sequence of events as the stem and conical nose piece are pushed forward. Up to the point at which the nose piece just touches the detached shock there is no fear of any oscillation. As soon as the nose piece tries to move through the shock there is a chance of oscillation. Whether oscillation will occur now depends on the angle of the conical nose piece ; the smaller the angle the greater the likelihood of oscillation. With further forward movement of the stem a point is reached at which the flow becomes steady and is of the pattern depicted in Fig. 26. This suggests that the flow is unstable in the range of stem positions limited by the cone positions shown in Figs. 25 and 26 because the flow can be satisfied by neither a detached shock (Fig. 25) nor a separation of the flow from the nose piece (Fig. 26). For the greater cone angles this flow unsteadiness does not arise as no flow separation from the conical nose piece is necessary in order that flow round the shoulder of the body can take place. (Note the angle of inclination of the flow from the base of the cone in Fig. 14.) Thus the limits of this type of unstable flow are defined as from the position at which the point of the cone touches the detached shock to the position at which the flow pattern changes to a flow separation just aft of the tip of the cone.

Outside the range defined above a smaller oscillation, which is still audible, can be detected at least for certain stem extensions. This type of flow oscillation consists of an oscillation of the mixing zone bounding the dead-air space in front of the body and a consequent oscillation of the flow at the shoulder of the body. The reason for this oscillation is not obvious ; it gives a blurred image of the mixing zone and flow at the shoulder of the body in the Schlieren photograph of Fig. 13. It is suggested that the mixing zone acts as an air jet which can excite the natural frequency of the dead-air space ahead of the body. That the oscillation occurs in some instances and not in others indicates that the jet will only excite certain frequencies. These

frequencies must then be near to the natural frequencies of the dead-air space for excitation to take place. The mechanism of the excitation of this type of oscillation has not been investigated fully.

4.4. *Boundary-Layer Transition.*—Once the steady flow pattern of Fig. 15 is reached with the ogive nose piece there is a subsequent gradual change in pressures on the front face of the body as the stem is moved further forward. This change is shown in Tables 1, 5 and 6 and also shows as a change in drag coefficient in Fig. 4 ; it can be explained by the gradual change in state of the boundary layer at the point of flow separation as the stem moves forward. The change in slope of the drag curves at about $4\frac{1}{2}$ in. stem extension could be a result of the transition from a laminar to a turbulent boundary layer on the stem. This is borne out by the fact that the gradual separation from the stem in Fig. 15 is typical of a laminar layer whereas the well defined point of separation of Fig. 17 suggests a turbulent layer.

4.5. *Pressure Measurements.*—The pressures on the face of the body were independent of the direction of movement of the stem except for a range of stem lengths the limits of which are given in the tables and denoted in Figs. 5 to 7 by vertical dashed lines. Within these limits the flow can be either of two configurations. If the stem is moving forwards the flow is of the type shown in Fig. 18 up to the forward limit when it changes suddenly to the type shown in Fig. 21. When the stem is withdrawn the flow does not revert to the original flow until a much shorter stem extension is reached (*cf.* Figs. 18 and 23).

4.6. *Drag Coefficients.*—Comparison of the derived drag coefficients plotted in Figs. 4 to 7 shows that the lowest drag is achieved with the 15 deg semi-angle nose piece at $M = 1{\cdot}6$ and $M = 1{\cdot}8$ ; at $M = 1{\cdot}5$ the 15 deg semi-angle nose piece is little better than the 30 deg, but this may be due to the length of the nose piece in the first case being so short as to allow the flow to change to the higher drag configuration before the real minimum could be reached. It should be possible to delay the change of flow pattern by lengthening the nose piece. The drag of the body with the ogive nose piece (Fig. 4) at high stem extensions has been neglected as being structurally unsound for application although it gives quite low drag coefficients.

The minimum drag coefficient of the body with the 15 deg semi-angle nose piece at $M = 1{\cdot}6$ (Fig. 5) is approximately equal to $0{\cdot}27$ for a stem extension of $3{\cdot}0$ in. If, however, the range of hysteresis is to be avoided the minimum $C_D$ is now approximately equal to $0{\cdot}31$ for a stem extension of $2{\cdot}0$ in. It would seem advisable, in practice, to avoid the region of hysteresis if possible to prevent the flow changing to the high drag configuration which might happen if the body were liable to changes of incidence. It would also seem advisable to avoid the range of stem extensions for which the main flow oscillation occurs. Since the stem position at which the flow pattern changes depends on the length of the nose piece, the present results cover a limited field. Further, the flow separation will presumably be a function of Reynolds number. However, with the understanding of the flow that has been gained from the results, it should be fairly easy to apply this method of reducing the drag of a bluff body to particular cases.

5. *Conclusions.*—The following main conclusions were reached as a result of a limited test programme in a supersonic wind tunnel to study the change in the flow over a bluff body caused by having a protruding stem and nose piece ahead of it. The tests, at $M = 1{\cdot}5$, $1{\cdot}6$ and $1{\cdot}8$, comprised pressure measurements on the front face of a square-ended, $1\frac{1}{2}$ in. diameter cylinder, and Schlieren observation, for a range of stem extensions with different shaped nose pieces.

5.1. The drag of the cylinder was reduced considerably by having a stem and conical nose piece projecting ahead of it. The tests indicated that the minimum drag coefficient was obtained with a 15 deg semi-angle conical nose piece which gave minimum drag coefficients of $0{\cdot}47$, $0{\cdot}27$ and $0{\cdot}21$ at $M = 1{\cdot}5$, $1{\cdot}6$ and $1{\cdot}8$ and corresponding stem projections of $2{\cdot}5$ in., $3{\cdot}25$ in. and

3·40 in. The equivalent conical heads to give the same drag coefficients are approximately 22½ deg, 16½ deg, 15 deg semi-angles. The drag coefficients of the blunt cylinder alone were 1·41, 1·41 and 1·47.

5.2. The drag of the cylinder alone was noted to be less than the drag of an open-ended tube of the same external dimensions.

5.3. The extent of the over-expansion bubble at the shoulder of the cylinder varied with movement of the stem and nose piece, within certain limits.

5.4. Certain stem extensions and nose pieces caused considerable main flow unsteadiness, the tendency for the onset of unsteadiness decreasing with increasing cone angle of the nose piece. For 30 deg and 40 deg semi-angle conical nose pieces the unsteadiness was completely avoided.

5.5. A less severe flow unsteadiness than the one mentioned above in paragraph 5.4 was also apparent, which caused an oscillation of the mixing zone coming from the base of the nose piece.

5.6. The two flow oscillations of sections 5.4 and 5.5 are considered to be similar to some oscillations experienced in the operation of centre-body intakes at supersonic speeds.

TABLE 1

*Pressures on Front Face of Bluff Body with Stem and Ogive Nose at* $M = 1{\cdot}5$

*Stagnation Pressure* $p_0 = 29{\cdot}81$ *in. Hg*

Stem extending

| $\frac{x}{}$ (in.) | $\frac{p_1}{p_0}$ | $\frac{p_2}{p_0}$ | $\frac{p_3}{p_0}$ |
|---|---|---|---|
| 0 | 0·843 | 0·903 | 0·923 |
| ¼ | 0·844 | 0·903 | 0·924 |
| ½ | 0·848 | 0·877 | 0·881 |
| ¾ | 0·849 | 0·873 | 0·887 |
| 1 | 0·851 | 0·865 | 0·868 |
| 1¼ | 0·814 | 0·845 | 0·846 |
| 1½ | 0·783 | 0·795 | 0·791 |
| 1¾ | 0·749 | 0·743 | 0·731 |
| 2 | | Unsteady flow | |
| 2¼ | | Unsteady flow | |
| 2½ | 0·589 | 0·508 | 0·515 |
| 2¾ | 0·584 | 0·501 | 0·507 |
| 3 | 0·581 | 0·502 | 0·506 |
| 3¼ | 0·575 | 0·498 | 0·503 |
| 3½ | 0·568 | 0·493 | 0·501 |
| 3¾ | 0·573 | 0·506 | 0·514 |
| 4 | 0·573 | 0·506 | 0·512 |
| 4¼ | 0·566 | 0·502 | 0·513 |
| 4½ | 0·557 | 0·497 | 0·511 |
| 4¾ | 0·538 | 0·491 | 0·507 |
| 5 | 0·516 | 0·486 | 0·504 |
| 5¼ | 0·495 | 0·478 | 0·496 |
| 5½ | 0·482 | 0·470 | 0·487 |
| 5¾ | 0·478 | 0·463 | 0·478 |
| 6 | 0·477 | 0·458 | 0·471 |
| 6¼ | 0·472 | 0·451 | 0·462 |
| 6½ | 0·468 | 0·444 | 0·455 |
| 6¾ | 0·462 | 0·438 | 0·450 |
| 7 | 0·454 | 0·430 | 0·444 |

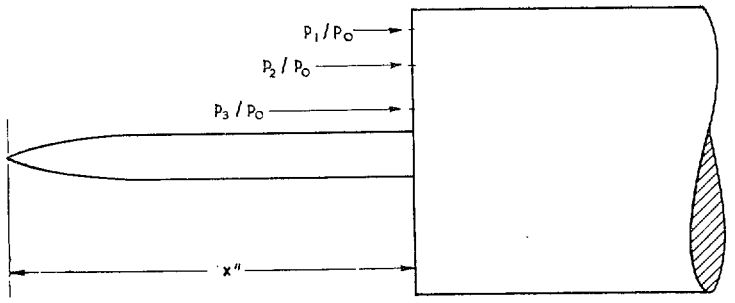


Stem receding

| $\frac{x}{}$ (in.) | $\frac{p_1}{p_0}$ | $\frac{p_2}{p_0}$ | $\frac{p_3}{p_0}$ |
|---|---|---|---|
| 4 | 0·569 | 0·504 | 0·514 |
| 3¾ | 0·570 | 0·504 | 0·512 |
| 3½ | 0·565 | 0·490 | 0·498 |
| 3¼ | 0·576 | 0·497 | 0·502 |
| 3 | 0·579 | 0·498 | 0·503 |

## TABLE 2

*Pressures on Front Face of Bluff Body with Stem and* 15 *deg Semi-angle Cone at* $M = 1{\cdot}5$

*Stagnation Pressure* $p_0 = 29{\cdot}76$ *in. Hg*

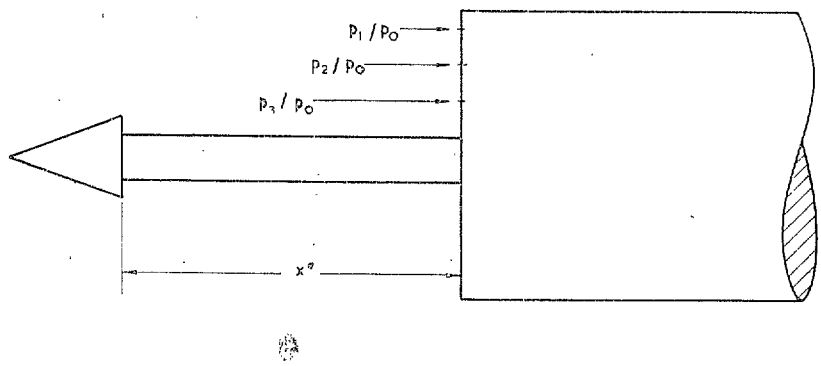


Stem extending

| $\frac{x}{}$ (in.) | $\frac{p_1}{p_0}$ | $\frac{p_2}{p_0}$ | $\frac{p_3}{p_0}$ |
|---|---|---|---|
| $\frac{1}{4}$ | 0·851 | 0·891 | 0·882 |
| $\frac{1}{2}$ | 0·864 | 0·828 | 0·820 |
| $\frac{3}{4}$ | 0·794 | 0·739 | 0·731 |
| 1 | 0·723 | 0·642 | 0·639 |
| $1\frac{1}{4}$ | 0·672 | 0·591 | 0·588 |
| $1\frac{1}{2}$ | 0·655 | 0·591 | 0·582 |
| $1\frac{3}{4}$ | 0·631 | 0·570 | 0·566 |
| 2 | 0·573 | 0·502 | 0·508 |
| $2\frac{1}{4}$ | 0·512 | 0·442 | 0·457 |
| $2\frac{1}{2}$ | | Flow changes | |
| $2\frac{3}{4}$ | 0·525 | 0·453 | 0·480 |
| 3 | 0·506 | 0·445 | 0·471 |
| $3\frac{1}{4}$ | 0·491 | 0·439 | 0·465 |
| $3\frac{1}{2}$ | 0·479 | 0·435 | 0·462 |
| $3\frac{3}{4}$ | 0·481 | 0·433 | 0·459 |
| 4 | 0·470 | 0·430 | 0·457 |

Stem receding

| $\frac{x}{}$ (in.) | $\frac{p_1}{p_0}$ | $\frac{p_2}{p_0}$ | $\frac{p_3}{p_0}$ |
|---|---|---|---|
| $3\frac{1}{2}$ | 0·492 | 0·435 | 0·461 |
| 3 | 0·529 | 0·445 | 0·471 |
| $2\frac{1}{2}$ | 0·573 | 0·464 | 0·491 |
| $2\frac{1}{4}$ | 0·605 | 0·481 | 0·509 |
| 2 | 0·566 | 0·494 | 0·499 |
| $1\frac{1}{2}$ | 0·644 | 0·581 | 0·574 |

Flow changes at
2·5 (advancing) and
2·05 (receding)

## TABLE 3

*Pressures on Front Face of Bluff Body with Stem and 30 deg Semi-angle Cone at $M = 1{\cdot}5$*
*Stagnation Pressure $p_0 = 29{\cdot}77$ in. Hg*

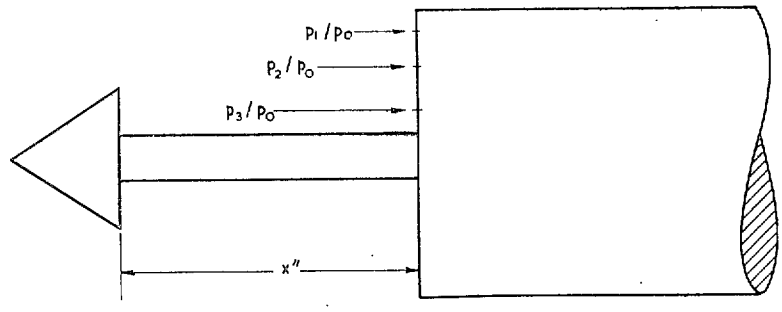


Stem extending

| $\frac{x}{}$ (in.) | $\frac{p_1}{p_0}$ | $\frac{p_2}{p_0}$ | $\frac{p_3}{p_0}$ |
|---|---|---|---|
| $\frac{1}{4}$ | 0·847 | 0·811 | 0·813 |
| $\frac{1}{2}$ | 0·7 | 0·668 | 0·681 |
| $\frac{3}{4}$ | 0·570 | 0·473 | 0·524 |
| 1 | 0·515 | 0·414 | 0·462 |
| $1\frac{1}{4}$ | 0·478 | 0·390 | 0·428 |
| $1\frac{1}{2}$ | 0·467 | 0·382 | 0·412 |
| $1\frac{3}{4}$ | 0·457 | 0·380 | 0·403 |
| 2 | 0·445 | 0·374 | 0·394 |
| $2\frac{1}{4}$ | 0·430 | 0·364 | 0·385 |
| $2\frac{1}{2}$ | 0·412 | 0·353 | 0·373 |
| $2\frac{3}{4}$ | 0·404 | 0·349 | 0·369 |
| 3 | 0·393 | 0·346 | 0·363 |
| $3\frac{1}{4}$ | 0·377 | 0·335 | 0·356 |
| $3\frac{1}{2}$ | 0·361 | 0·329 | 0·351 |
| $3\frac{3}{4}$ | 0·359 | 0·331 | 0·352 |
| 4 | 0·365 | 0·339 | 0·357 |
| $4\frac{1}{4}$ | 0·378 | 0·349 | 0·366 |
| $4\frac{1}{2}$ | 0·401 | 0·369 | 0·384 |
| $4\frac{3}{4}$ | 0·544 | 0·493 | 0·506 |
| 5 | 0·545 | 0·492 | 0·504 |
| $5\frac{1}{4}$ | 0·545 | 0·491 | 0·502 |
| $5\frac{1}{2}$ | 0·541 | 0·488 | 0·501 |

Stem receding

| $\frac{x}{}$ (in.) | $\frac{p_1}{p_0}$ | $\frac{p_2}{p_0}$ | $\frac{p_3}{p_0}$ |
|---|---|---|---|
| $5\frac{1}{4}$ | 0·545 | 0·490 | 0·502 |
| 5 | 0·543 | 0·492 | 0·504 |
| $4\frac{3}{4}$ | 0·543 | 0·493 | 0·506 |
| $4\frac{1}{2}$ | 0·543 | 0·493 | 0·506 |
| $4\frac{1}{4}$ | 0·538 | 0·492 | 0·507 |
| 4 | 0·528 | 0·489 | 0·504 |
| $3\frac{3}{4}$ | 0·360 | 0·331 | 0·351 |
| $3\frac{1}{2}$ | 0·361 | 0·327 | 0·349 |
| $3\frac{1}{4}$ | 0·372 | 0·329 | 0·350 |
| 3 | 0·388 | 0·336 | 0·357 |

Flow changes at
4·6 in. extending and
3·9 in. receding

TABLE 4

*Pressures on Front Face of Bluff Body with Stem and 40 deg Semi-angle Cone at* $M = 1{\cdot}5$
*Stagnation Pressure* $p_0 = 29{\cdot}78$ *in. Hg*

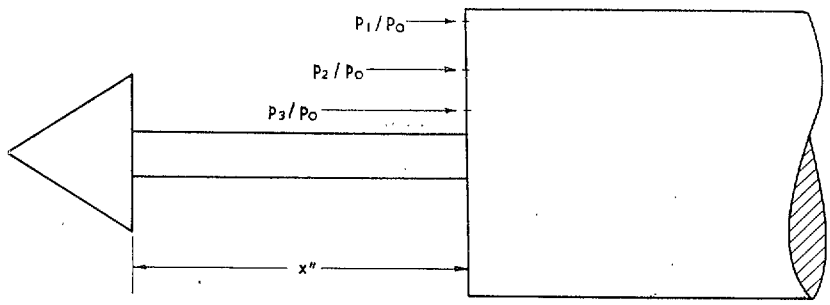


Stem extending

| $\frac{x}{\text{(in.)}}$ | $\frac{p_1}{p_0}$ | $\frac{p_2}{p_0}$ | $\frac{p_3}{p_0}$ |
|---|---|---|---|
| 3 | 0·325 | 0·292 | 0·317 |
| 6 | 0·372 | 0·366 | 0·376 |

## TABLE 5

*Pressures on Front Face of Bluff Body with Stem and Ogive Nose at $M = 1{\cdot}6$*
*Stagnation Pressure $p_0 = 29{\cdot}88$ in. Hg*

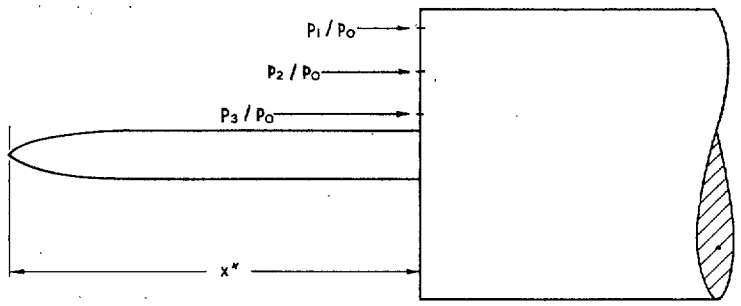


Stem extending

| $\frac{x}{}$ (in.) | $\frac{p_1}{p_0}$ | $\frac{p_2}{p_0}$ | $\frac{p_3}{p_0}$ |
|---|---|---|---|
| 0 | 0·805 | 0·863 | 0·883 |
| $\frac{1}{4}$ | 0·806 | 0·863 | 0·883 |
| $\frac{1}{2}$ | 0·811 | 0·868 | 0·845 |
| $\frac{3}{4}$ | 0·811 | 0·868 | 0·846 |
| 1 | 0·781 | 0·830 | 0·844 |
| $1\frac{1}{4}$ | 0·763 | 0·800 | 0·812 |
| $1\frac{1}{2}$ | 0·730 | 0·754 | 0·761 |
| $1\frac{3}{4}$ | 0·710 | 0·719 | 0·714 |
| 2 | 0·498 | 0·413 | 0·436 |
| $2\frac{1}{4}$ | 0·503 | 0·413 | 0·432 |
| $2\frac{1}{2}$ | 0·502 | 0·412 | 0·428 |
| $2\frac{3}{4}$ | 0·500 | 0·412 | 0·427 |
| 3 | 0·501 | 0·421 | 0·431 |
| $3\frac{1}{4}$ | 0·499 | 0·418 | 0·428 |
| $3\frac{1}{2}$ | 0·498 | 0·415 | 0·427 |
| $3\frac{3}{4}$ | 0·519 | 0·434 | 0·444 |
| 4 | 0·520 | 0·435 | 0·444 |
| $4\frac{1}{4}$ | 0·522 | 0·435 | 0·446 |
| $4\frac{1}{2}$ | 0·531 | 0·434 | 0·448 |
| $4\frac{3}{4}$ | 0·540 | 0·435 | 0·448 |
| 5 | 0·538 | 0·435 | 0·447 |
| $5\frac{1}{4}$ | 0·534 | 0·434 | 0·447 |
| $5\frac{1}{2}$ | 0·533 | 0·434 | 0·449 |
| $5\frac{3}{4}$ | 0·492 | 0·419 | 0·437 |
| 6 | 0·460 | 0·406 | 0·425 |
| $6\frac{1}{4}$ | 0·441 | 0·399 | 0·415 |
| $6\frac{1}{2}$ | 0·431 | 0·394 | 0·405 |
| $6\frac{3}{4}$ | 0·423 | 0·390 | 0·399 |
| 7 | 0·416 | 0·384 | 0·391 |

## TABLE 6

*Pressures on Front Face of Bluff Body with Stem and* 15 *deg Semi-angle Cone at* $M = 1{\cdot}6$
*Stagnation Pressure* $p_0 = 29{\cdot}87$ *in. Hg*

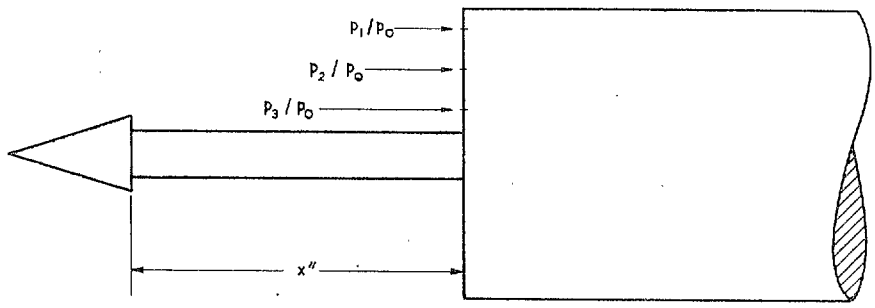


Stem extending

| $\frac{x}{}$ (in.) | $\frac{p_1}{p_0}$ | $\frac{p_2}{p_0}$ | $\frac{p_3}{p_0}$ |
|---|---|---|---|
| $\frac{1}{4}$ | 0·815 | 0·846 | 0·828 |
| $\frac{1}{2}$ | 0·792 | 0·781 | 0·772 |
| $\frac{3}{4}$ | 0·711 | 0·674 | 0·662 |
| 1 | 0·645 | 0·582 | 0·577 |
| $1\frac{1}{4}$ | 0·574 | 0·484 | 0·494 |
| $1\frac{1}{2}$ | 0·558 | 0·478 | 0·483 |
| $1\frac{3}{4}$ | 0·537 | 0·456 | 0·463 |
| 2 | 0·380 | 0·338 | 0·364 |
| $2\frac{1}{4}$ | 0·380 | 0·334 | 0·359 |
| $2\frac{1}{2}$ | 0·384 | 0·331 | 0·354 |
| $2\frac{3}{4}$ | 0·364 | 0·319 | 0·344 |
| 3 | 0·370 | 0·319 | 0·343 |
| $3\frac{1}{4}$ | 0·460 | 0·384 | 0·411 |
| $3\frac{1}{2}$ | 0·453 | 0·380 | 0·407 |
| $3\frac{3}{4}$ | 0·452 | 0·377 | 0·405 |
| 4 | 0·452 | 0·374 | 0·402 |
| $4\frac{1}{4}$ | 0·448 | 0·369 | 0·397 |

Stem receding

| $\frac{x}{}$ (in.) | $\frac{p_1}{p_0}$ | $\frac{p_2}{p_0}$ | $\frac{p_3}{p_0}$ |
|---|---|---|---|
| 4 | 0·448 | 0·373 | 0·400 |
| $3\frac{1}{2}$ | 0·449 | 0·379 | 0·407 |
| 3 | 0·465 | 0·388 | 0·416 |
| $2\frac{3}{4}$ | 0·473 | 0·397 | 0·422 |
| $2\frac{1}{2}$ | 0·485 | 0·403 | 0·429 |
| $2\frac{1}{4}$ | 0·516 | 0·417 | 0·445 |
| 2 | 0·378 | 0·336 | 0·363 |
| $1\frac{1}{2}$ | 0·556 | 0·476 | 0·480 |

Flow changes at
3·25 in. extending and
2·0 in. receding

## TABLE 7

*Pressures on Front Face of Bluff Body with Stem and 30 deg Semi-angle Cone at $M = 1{\cdot}6$*
*Stagnation Pressure $p_0 = 29{\cdot}74$ in. Hg*

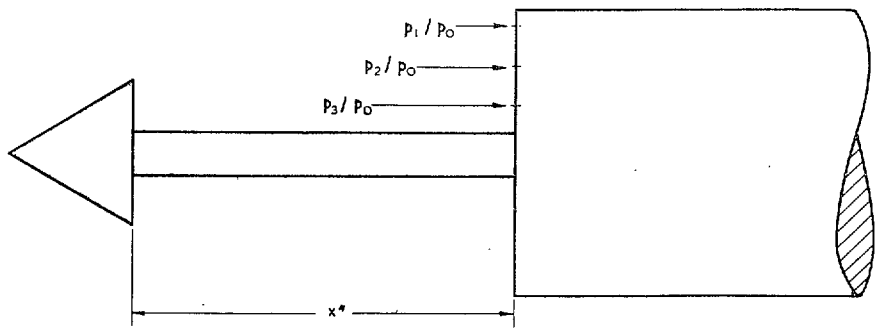


Stem extending

| $x$ (in.) | $p_1/p_0$ | $p_2/p_0$ | $p_3/p_0$ |
|---|---|---|---|
| $\frac{1}{4}$ | 0·824 | 0·786 | 0·787 |
| $\frac{1}{2}$ | 0·652 | 0·616 | 0·632 |
| $\frac{3}{4}$ | 0·513 | 0·419 | 0·471 |
| 1 | 0·438 | 0·358 | 0·400 |
| $1\frac{1}{4}$ | 0·424 | 0·337 | 0·371 |
| $1\frac{1}{2}$ | 0·411 | 0·330 | 0·359 |
| $1\frac{3}{4}$ | 0·396 | 0·322 | 0·348 |
| 2 | 0·376 | 0·310 | 0·336 |
| $2\frac{1}{4}$ | 0·356 | 0·299 | 0·323 |
| $2\frac{1}{2}$ | 0·343 | 0·292 | 0·316 |
| $2\frac{3}{4}$ | 0·333 | 0·286 | 0·310 |
| 3 | 0·320 | 0·280 | 0·303 |
| $3\frac{1}{4}$ | 0·312 | 0·276 | 0·299 |
| $3\frac{1}{2}$ | 0·318 | 0·278 | 0·301 |
| $3\frac{3}{4}$ | 0·326 | 0·284 | 0·304 |
| 4 | 0·336 | 0·293 | 0·310 |
| $4\frac{1}{4}$ | 0·351 | 0·304 | 0·320 |
| $4\frac{1}{2}$ | 0·508 | 0·436 | 0·446 |
| $4\frac{3}{4}$ | 0·507 | 0·433 | 0·444 |
| 5 | 0·490 | 0·427 | 0·441 |

Stem receding

| $x$ (in.) | $p_1/p_0$ | $p_2/p_0$ | $p_3/p_0$ |
|---|---|---|---|
| $4\frac{1}{2}$ | 0·510 | 0·436 | 0·446 |
| 4 | 0·512 | 0·439 | 0·450 |
| $3\frac{1}{2}$ | 0·319 | 0·278 | 0·301 |
| 3 | 0·319 | 0·280 | 0·304 |
| $2\frac{1}{2}$ | 0·342 | 0·292 | 0·315 |

Flow changes at
4·5 in. extending and
3·6 in. receding

## TABLE 8

*Pressures on Front Face of Bluff Body with Stem and* 40 *deg Semi-angle Cone at* $M = 1{\cdot}6$
*Stagnation Pressure* $p_0 = 29{\cdot}71$ *in. Hg*

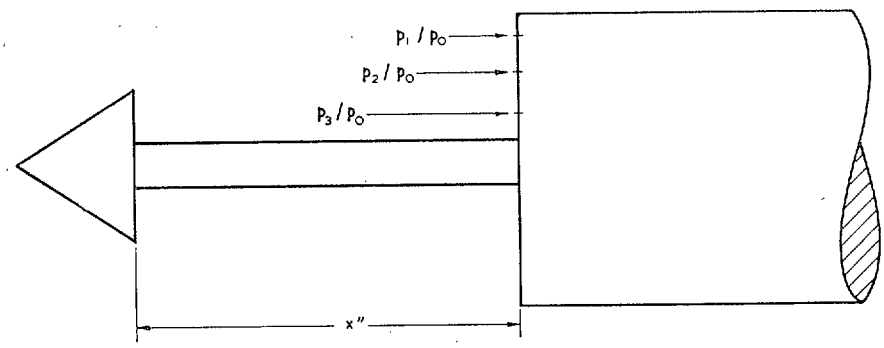


Stem extending

| $\frac{x}{\text{(in.)}}$ | $\frac{p_1}{p_0}$ | $\frac{p_2}{p_0}$ | $\frac{p_3}{p_0}$ |
|---|---|---|---|
| 1 | 0·237 | 0·232 | 0·252 |
| 2 | 0·264 | 0·232 | 0·262 |
| 3 | 0·256 | 0·239 | 0·264 |
| 4 | 0·271 | 0·249 | 0·271 |
| 5 | 0·312 | 0·284 | 0·295 |
| $5\frac{1}{2}$ | 0·484 | 0·446 | 0·441 |
| 6 | 0·483 | 0·450 | 0·450 |

Stem receding

| $\frac{x}{\text{(in.)}}$ | $\frac{p_1}{p_0}$ | $\frac{p_2}{p_0}$ | $\frac{p_3}{p_0}$ |
|---|---|---|---|
| 5 | 0·317 | 0·287 | 0·298 |
| 4 | 0·271 | 0·250 | 0·272 |

Flow changes at
5·5 in. extending and
5·1 in. receding

TABLE 9

*Pressures on Front Face of Bluff Body with Stem and Ogive Nose at* $M = 1{\cdot}8$

*Stagnation Pressure* $p_0 = 30{\cdot}00$ *in. Hg*

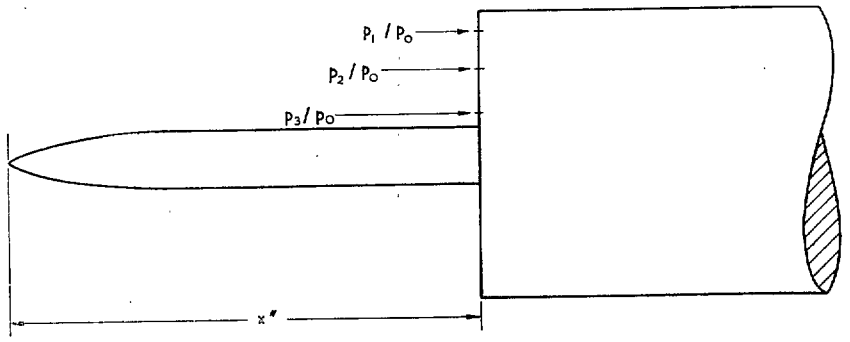


Stem extending

| $\frac{x}{\text{(in.)}}$ | $\frac{p_1}{p_0}$ | $\frac{p_2}{p_0}$ | $\frac{p_3}{p_0}$ |
|---|---|---|---|
| 0 | 0·731 | 0·784 | 0·802 |
| $\frac{1}{4}$ | 0·731 | 0·784 | 0·803 |
| $\frac{1}{2}$ | 0·737 | 0·789 | 0·768 |
| $\frac{3}{4}$ | 0·738 | 0·789 | 0·771 |
| 1 | 0·703 | 0·749 | 0·785 |
| $1\frac{1}{4}$ | 0·682 | 0·724 | 0·743 |
| $1\frac{1}{2}$ | 0·664 | 0·685 | 0·697 |
| $1\frac{3}{4}$ | 0·641 | 0·655 | 0·657 |
| 2 | 0·420 | 0·319 | 0·344 |
| $2\frac{1}{4}$ | 0·399 | 0·306 | 0·328 |
| $2\frac{1}{2}$ | 0·411 | 0·312 | 0·330 |
| $2\frac{3}{4}$ | 0·411 | 0·312 | 0·329 |
| 3 | 0·408 | 0·315 | 0·330 |
| $3\frac{1}{4}$ | 0·405 | 0·315 | 0·329 |
| $3\frac{1}{2}$ | 0·404 | 0·315 | 0·327 |
| $3\frac{3}{4}$ | 0·408 | 0·318 | 0·329 |
| 4 | 0·416 | 0·329 | 0·338 |
| $4\frac{1}{4}$ | 0·415 | 0·330 | 0·338 |
| $4\frac{1}{2}$ | 0·415 | 0·331 | 0·338 |
| $4\frac{3}{4}$ | 0·415 | 0·330 | 0·338 |
| 5 | 0·410 | 0·330 | 0·337 |

Stem receding

| $\frac{x}{\text{(in.)}}$ | $\frac{p_1}{p_0}$ | $\frac{p_2}{p_0}$ | $\frac{p_3}{p_0}$ |
|---|---|---|---|
| $3\frac{1}{2}$ | 0·406 | 0·317 | 0·329 |

## TABLE 10

*Pressures on Front Face of Bluff Body with Stem and* 15 *deg Semi-angle Cone at* $M = 1{\cdot}8$
*Stagnation Pressure* $p_0 = 30{\cdot}04$ *in. Hg*

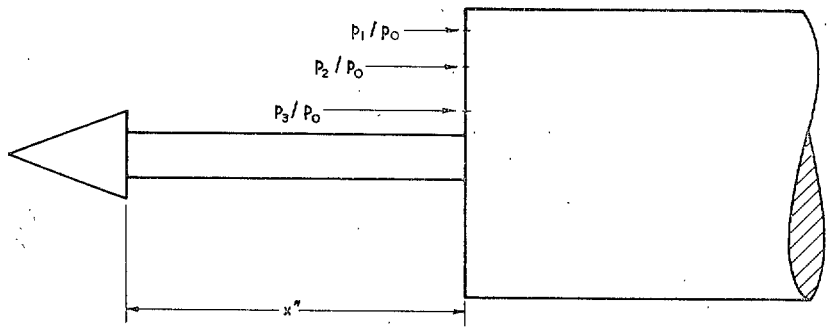


Stem extending

| $\frac{x}{\text{(in.)}}$ | $\frac{p_1}{p_0}$ | $\frac{p_2}{p_0}$ | $\frac{p_3}{p_0}$ |
|---|---|---|---|
| 0 | 0·736 | 0·790 | 0·781 |
| $\frac{1}{4}$ | 0·717 | 0·766 | 0·762 |
| $\frac{1}{2}$ | 0·699 | 0·676 | 0·668 |
| $\frac{3}{4}$ | 0·629 | 0·596 | 0·584 |
| 1 | 0·566 | 0·507 | 0·503 |
| $1\frac{1}{4}$ | 0·459 | 0·373 | 0·390 |
| $1\frac{1}{2}$ | 0·432 | 0·356 | 0·371 |
| $1\frac{3}{4}$ | 0·401 | 0·327 | 0·341 |
| 2 | 0·347 | 0·269 | 0·292 |
| $2\frac{1}{4}$ | 0·333 | 0·258 | 0·279 |
| $2\frac{1}{2}$ | 0·326 | 0·254 | 0·272 |
| $2\frac{3}{4}$ | 0·322 | 0·253 | 0·269 |
| 3 | 0·321 | 0·255 | 0·268 |
| $3\frac{1}{4}$ | 0·324 | 0·259 | 0·271 |
| $3\frac{1}{2}$ | 0·400 | 0·309 | 0·327 |
| $3\frac{3}{4}$ | 0·395 | 0·306 | 0·324 |
| 4 | 0·393 | 0·302 | 0·319 |
| $4\frac{1}{4}$ | 0·389 | 0·302 | 0·317 |
| $4\frac{1}{2}$ | 0·384 | 0·298 | 0·308 |
| $4\frac{3}{4}$ | 0·377 | 0·296 | 0·307 |
| 5 | 0·378 | 0·294 | 0·307 |
| $5\frac{1}{4}$ | 0·374 | 0·294 | 0·305 |
| $5\frac{1}{2}$ | 0·370 | 0·293 | 0·303 |

Stem receding

| $\frac{x}{\text{(in.)}}$ | $\frac{p_1}{p_0}$ | $\frac{p_2}{p_0}$ | $\frac{p_3}{p_0}$ |
|---|---|---|---|
| 5 | 0·377 | 0·293 | 0·306 |
| $4\frac{1}{2}$ | 0·382 | 0·297 | 0·311 |
| 4 | 0·391 | 0·301 | 0·317 |
| $3\frac{1}{2}$ | 0·400 | 0·309 | 0·327 |
| 3 | 0·406 | 0·314 | 0·335 |
| $2\frac{1}{2}$ | 0·419 | 0·325 | 0·349 |
| $2\frac{1}{4}$ | 0·432 | 0·337 | 0·362 |
| 2 | 0·466 | 0·359 | 0·385 |
| $1\frac{3}{4}$ | 0·402 | 0·327 | 0·341 |
| $1\frac{1}{2}$ | 0·431 | 0·354 | 0·369 |
| 1 | 0·578 | 0·525 | 0·518 |

Flow changes at
3·4 in. extending and
1·9 in. receding

## TABLE 11

*Pressures on Front Face of Bluff Body with Stem and 30 deg Semi-angle Cone at* $M = 1{\cdot}8$

*Stagnation Pressure* $p_0 = 29{\cdot}66$ *in. Hg*

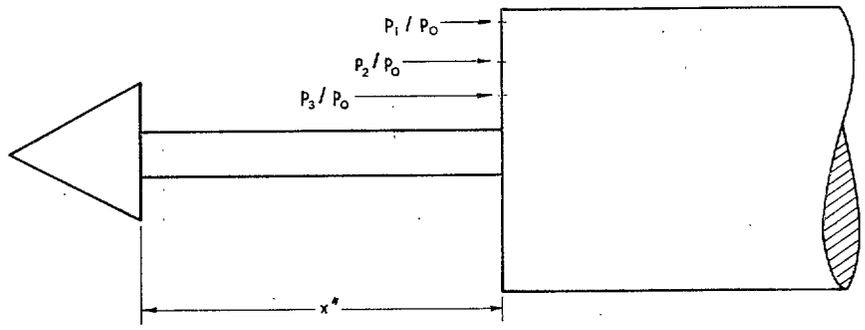


Stem extending

| $x$ (in.) | $\frac{p_1}{p_0}$ | $\frac{p_2}{p_0}$ | $\frac{p_3}{p_0}$ |
|---|---|---|---|
| $\frac{1}{4}$ | 0·749 | 0·748 | 0·747 |
| $\frac{1}{2}$ | 0·554 | 0·489 | 0·518 |
| $\frac{3}{4}$ | 0·423 | 0·347 | 0·388 |
| 1 | 0·358 | 0·288 | 0·324 |
| $1\frac{1}{4}$ | 0·343 | 0·265 | 0·296 |
| $1\frac{1}{2}$ | 0·324 | 0·251 | 0·279 |
| $1\frac{3}{4}$ | 0·306 | 0·236 | 0·260 |
| 2 | 0·297 | 0·228 | 0·255 |
| $2\frac{1}{4}$ | 0·283 | 0·220 | 0·245 |
| $2\frac{1}{2}$ | 0·270 | 0·212 | 0·236 |
| $2\frac{3}{4}$ | 0·267 | 0·211 | 0·232 |
| 3 | 0·267 | 0·231 | 0·231 |
| $3\frac{1}{4}$ | 0·269 | 0·218 | 0·233 |
| $3\frac{1}{2}$ | 0·271 | 0·222 | 0·234 |
| $3\frac{3}{4}$ | 0·273 | 0·224 | 0·235 |
| 4 | 0·276 | 0·229 | 0·238 |
| $4\frac{1}{4}$ | 0·285 | 0·238 | 0·245 |
| $4\frac{1}{2}$ | 0·413 | 0·336 | 0·347 |
| $4\frac{3}{4}$ | 0·415 | 0·335 | 0·344 |
| 5 | 0·396 | 0·335 | 0·341 |
| $5\frac{1}{4}$ | 0·420 | 0·330 | 0·342 |
| $5\frac{1}{2}$ | 0·407 | 0·327 | 0·335 |

Stem receding

| $x$ (in.) | $\frac{p_1}{p_0}$ | $\frac{p_2}{p_0}$ | $\frac{p_3}{p_0}$ |
|---|---|---|---|
| 5 | 0·395 | 0·334 | 0·341 |
| $4\frac{1}{2}$ | 0·415 | 0·340 | 0·347 |
| 4 | 0·407 | 0·350 | 0·356 |
| $3\frac{1}{2}$ | 0·457 | 0·366 | 0·367 |
| $3\frac{1}{4}$ | 0·270 | 0·218 | 0·233 |
| 3 | 0·268 | 0·215 | 0·233 |

Flow changes at
4·5 in. extending and
3·25 in. receding

## TABLE 12

*Pressures on Front Face of Bluff Body with Stem and 40 deg Semi-angle Cone at $M = 1{\cdot}8$*
*Stagnation Pressure $p_0 = 29{\cdot}67$ in. Hg*

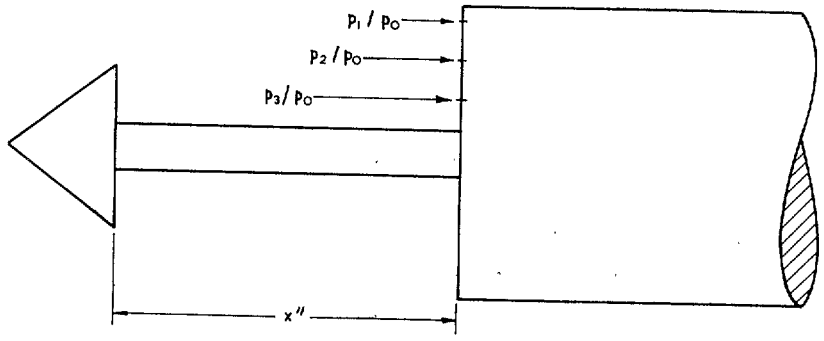


Stem extending

| $x$ (in.) | $p_1/p_0$ | $p_2/p_0$ | $p_3/p_0$ |
|---|---|---|---|
| 1 | 0·210 | 0·193 | 0·210 |
| 2 | 0·218 | 0·172 | 0·201 |
| 3 | 0·216 | 0·174 | 0·199 |
| 4 | 0·234 | 0·193 | 0·210 |
| 5 | 0·250 | 0·219 | 0·226 |
| $5\frac{1}{4}$ | 0·261 | 0·229 | 0·236 |
| $5\frac{1}{2}$ | 0·419 | 0·354 | 0·354 |
| 6 | 0·417 | 0·353 | 0·354 |

Stem receding

| $x$ (in.) | $p_1/p_0$ | $p_2/p_0$ | $p_3/p_0$ |
|---|---|---|---|
| 5 | 0·413 | 0·351 | 0·352 |
| $4\frac{3}{4}$ | 0·245 | 0·214 | 0·221 |
| 4 | 0·235 | 0·196 | 0·211 |

Flow changes at
5·5 in. advancing and
4·75 in. receding

## TABLE 13

*Pressures on Front Face of Bluff Body alone at $M = 1{\cdot}5$, $1{\cdot}6$ and $1{\cdot}8$*

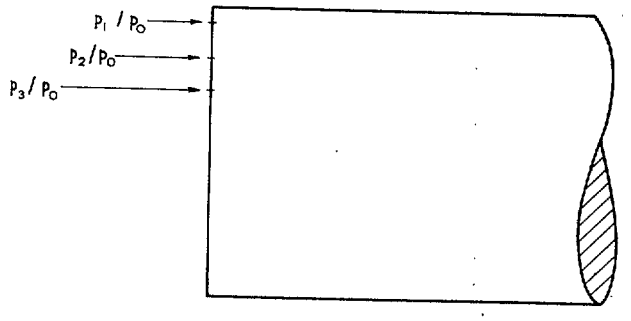


| $M$ | $p_1/p_0$ | $p_2/p_0$ | $p_3/p_0$ | $p_0'/p_0$ |
|---|---|---|---|---|
| 1·5 | 0·843 | 0·903 | 0·923 | 0·9298 |
| 1·6 | 0·805 | 0·863 | 0·883 | 0·8952 |
| 1·8 | 0·731 | 0·784 | 0·802 | 0·8127 |

$$\frac{p_0'}{p_0} = \frac{\text{pitot pressure}}{\text{stagnation pressure}}$$

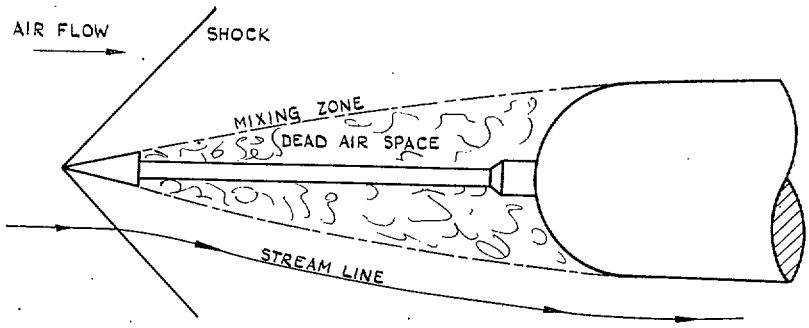


FIG. 1. Bluff body with conical windshield.

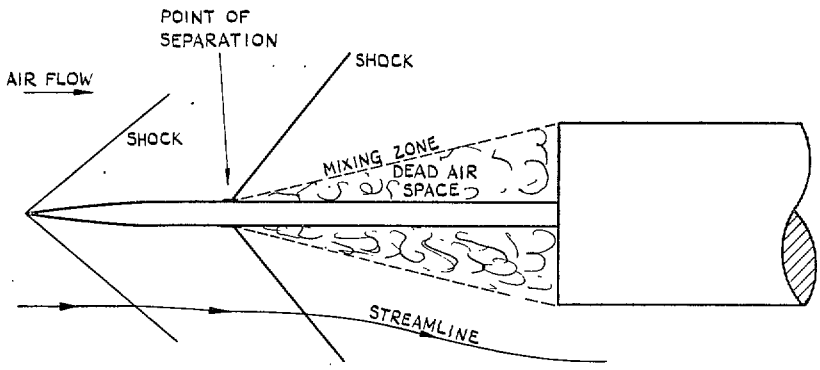


FIG. 2. Bluff body with spike.

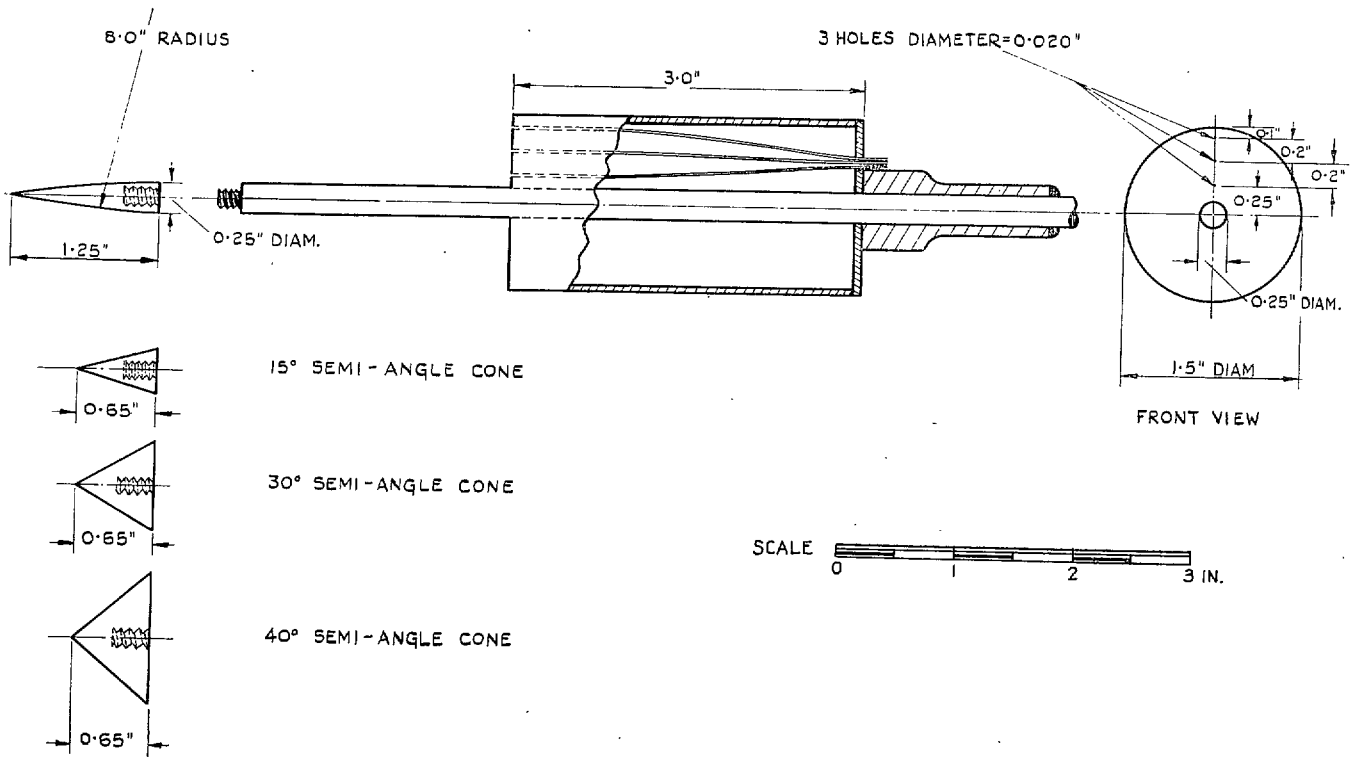


FIG. 3. Test arrangement with alternative nose pieces.

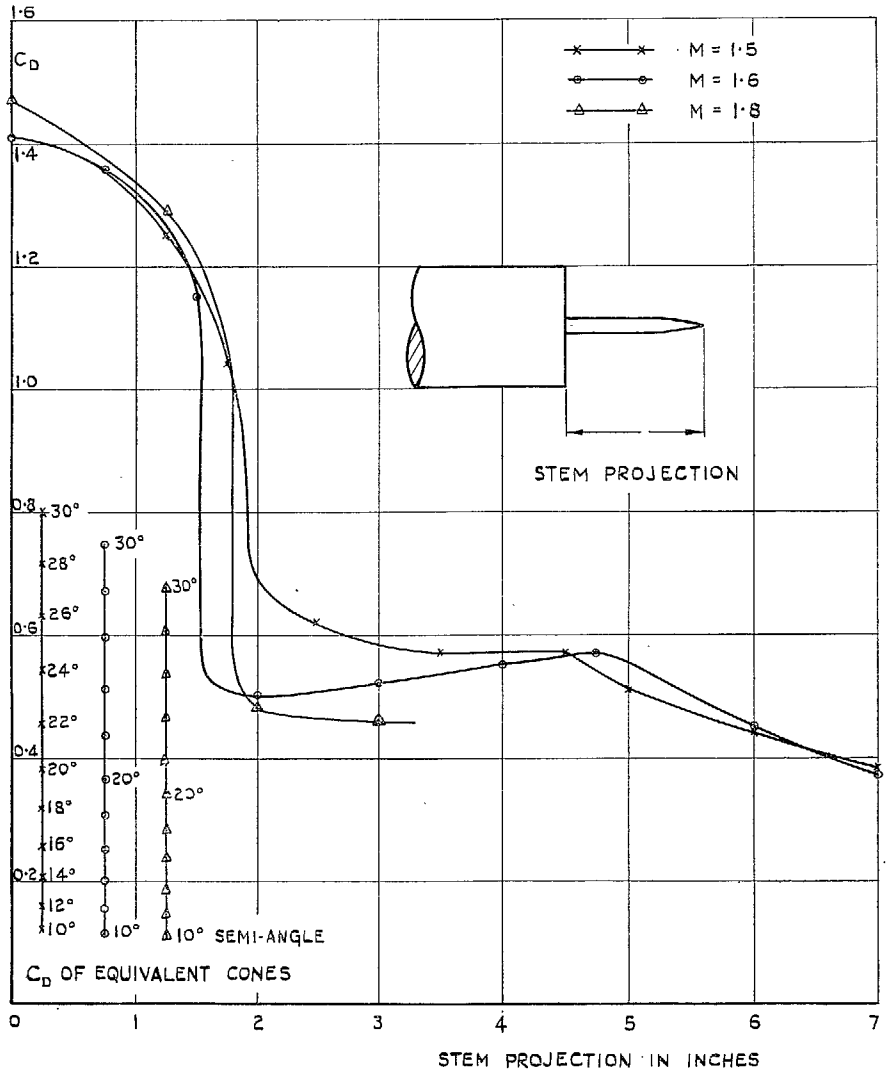


FIG. 4. Drag of bluff body with ogive nose mounted on stem.

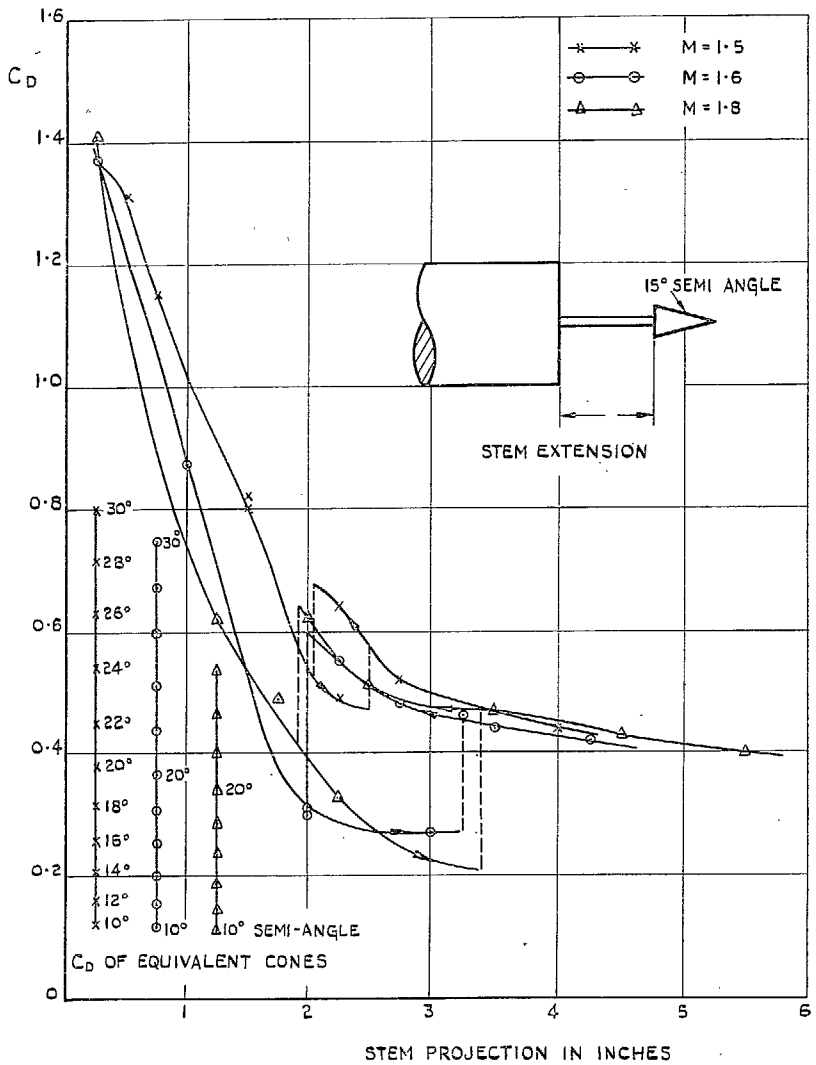


FIG. 5. Drag of bluff body with 15 deg semi-angle cone mounted on stem.

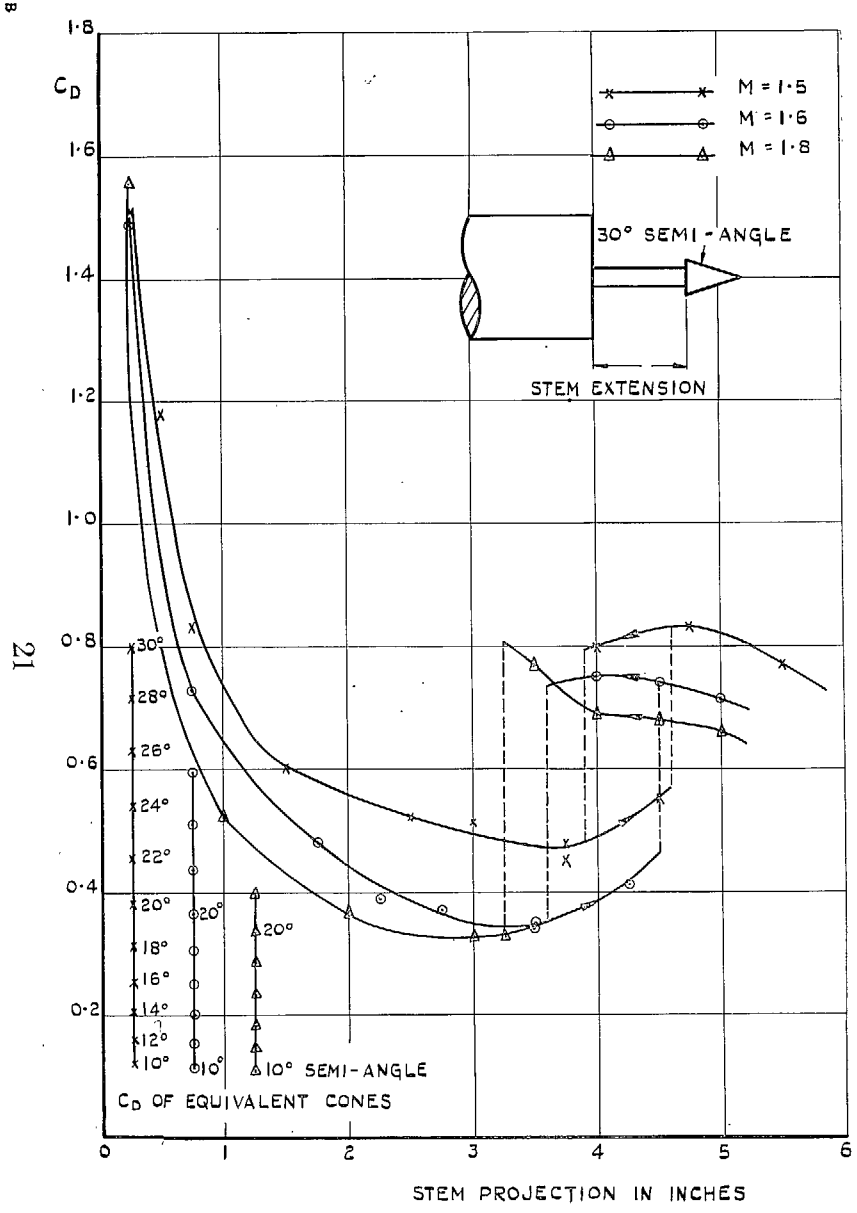


FIG. 6. Drag of bluff body with 30 deg semi-angle cone mounted on stem.

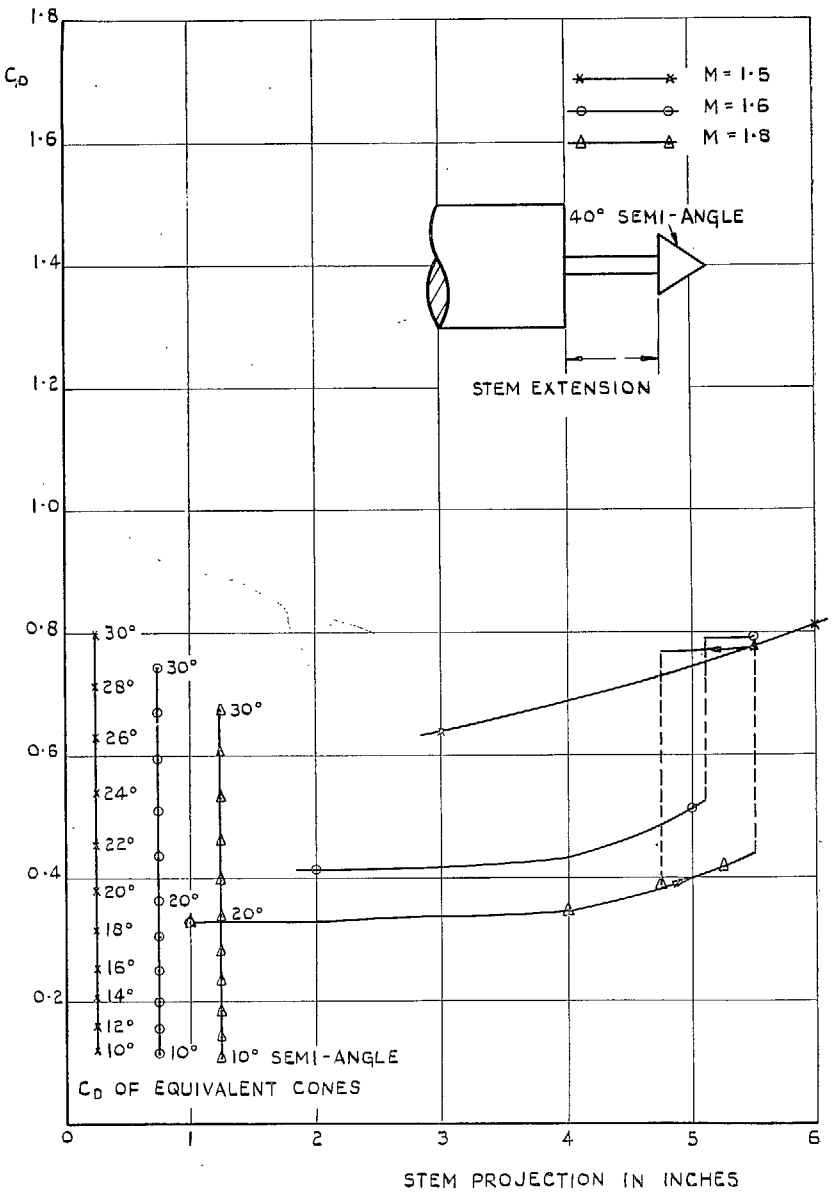


FIG. 7. Drag of bluff body with 40 deg semi-angle cone mounted on stem.

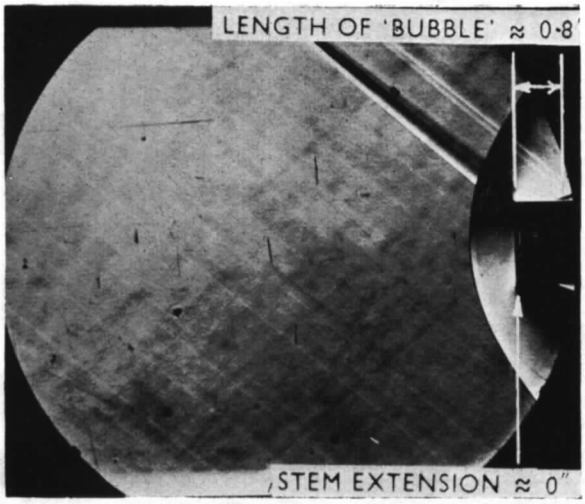


FIG. 8. Bluff body ($M = 1{\cdot}6$).

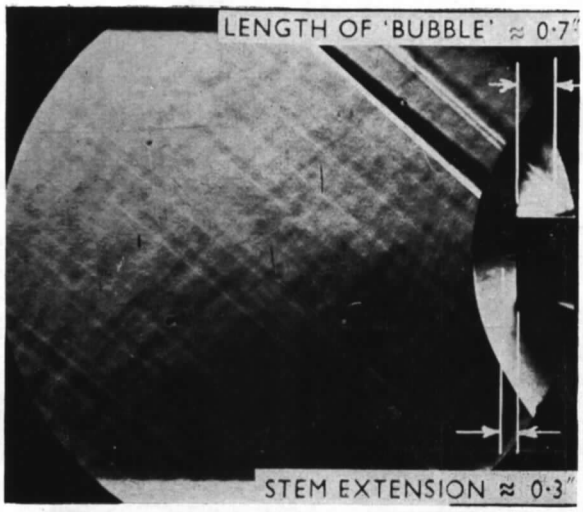


FIG. 9. Bluff body with stem and ogive nose ($M = 1{\cdot}6$).

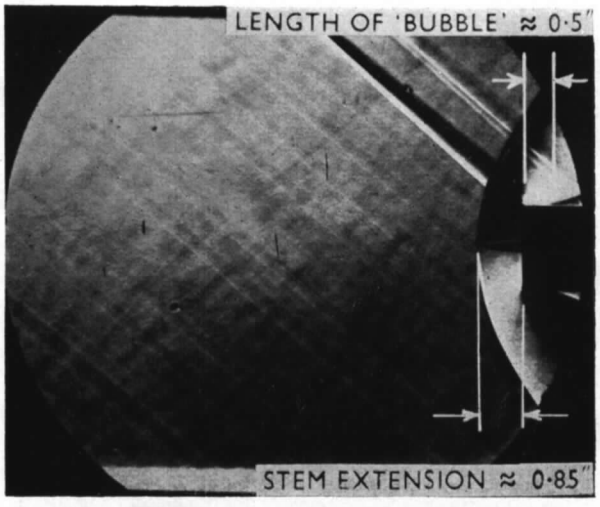


FIG. 10. Bluff body with stem and ogive nose ($M = 1{\cdot}6$).

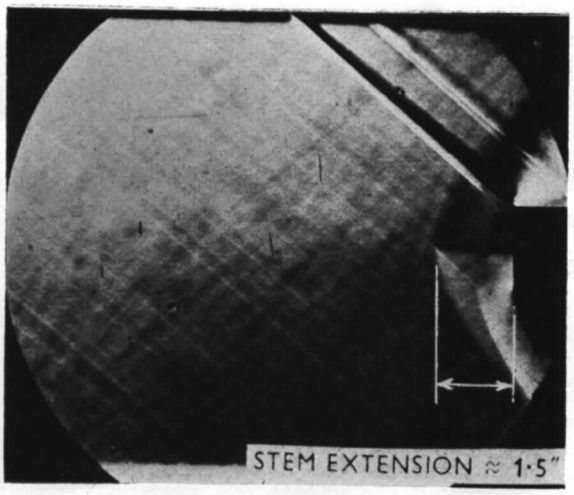


FIG. 11. Bluff body with stem and ogive nose ($M = 1 \cdot 6$) (shock oscillation).

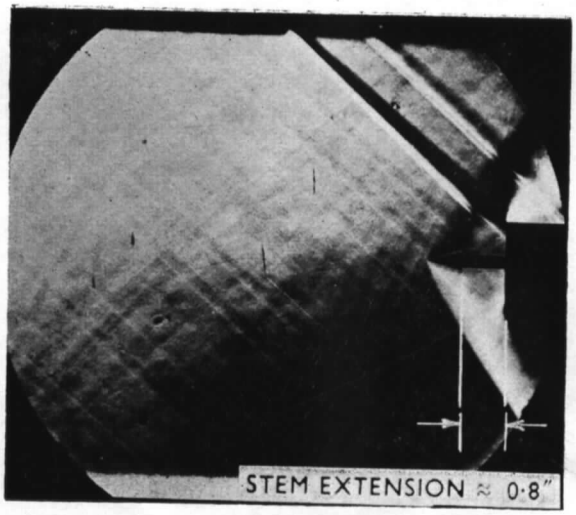


FIG. 12. Bluff body with stem and 15 deg semi-angle cone ($M = 1 \cdot 6$) (shock oscillation).

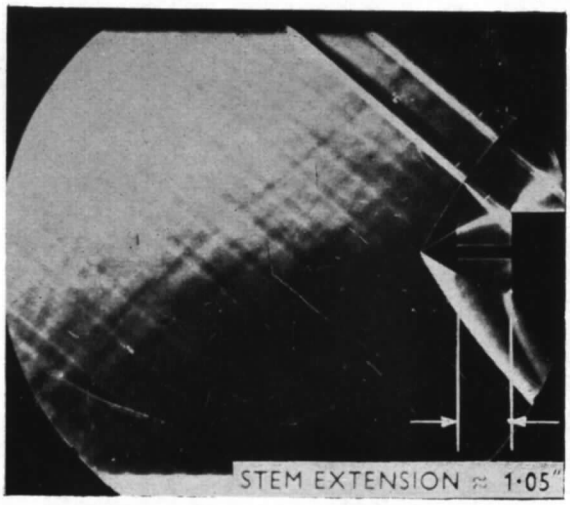


FIG. 13. Bluff body with stem and 30 deg semi-angle cone ($M = 1 \cdot 6$) (small oscillation of shock at shoulder of body).

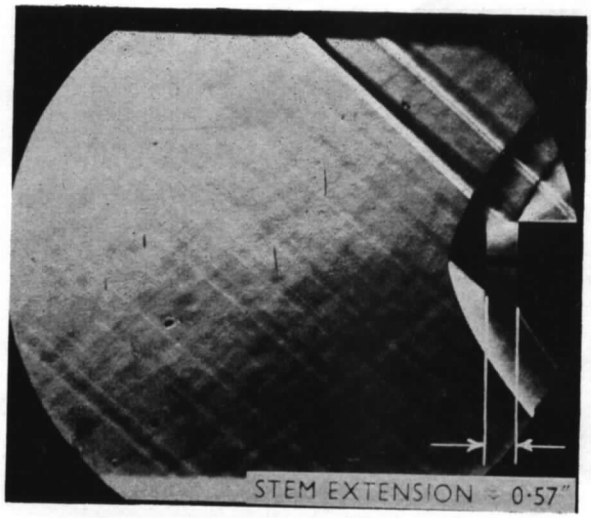


FIG. 14. Bluff body with stem and 40 deg semi-angle cone ($M = 1 \cdot 6$) (no oscillation).

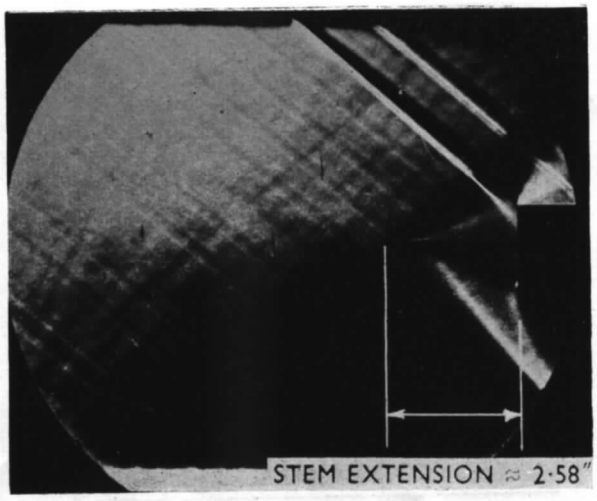


FIG. 15. Bluff body with stem and ogive nose ($M = 1{\cdot}6$).

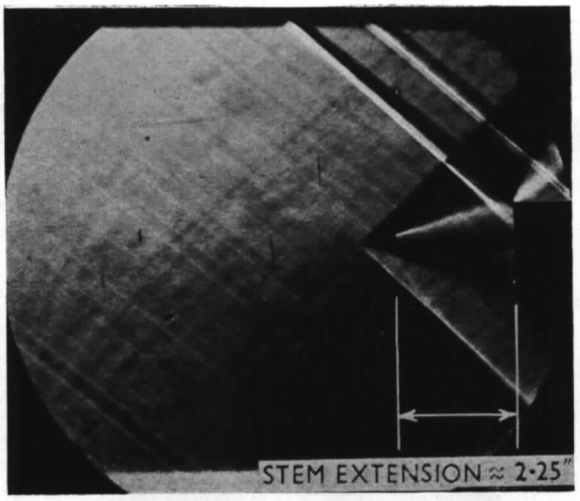


FIG. 16. Bluff body with stem and 15 deg semi-angle cone ($M = 1{\cdot}6$).

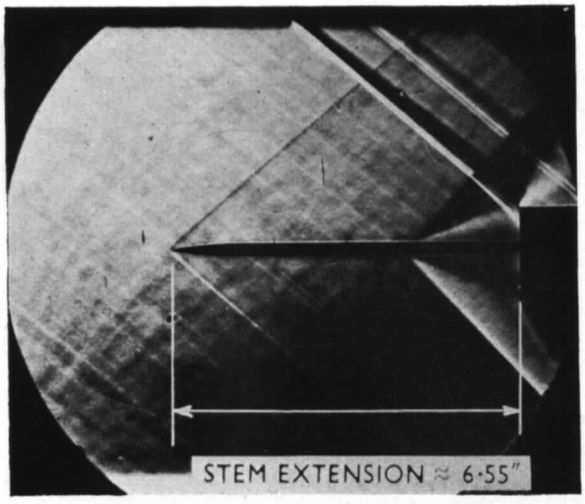


FIG. 17. Bluff body with stem and ogive nose ($M = 1{\cdot}6$).

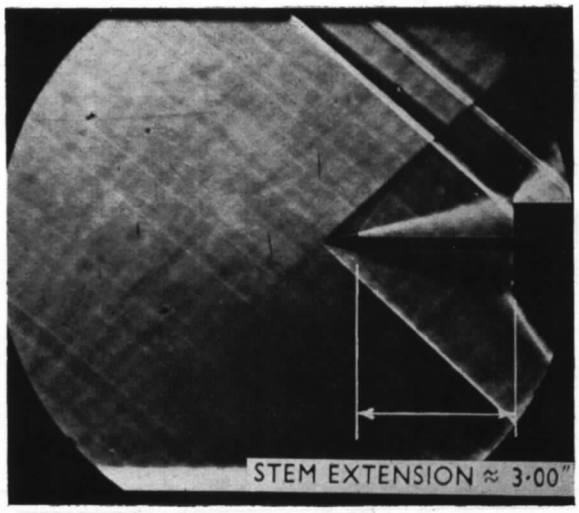


FIG. 18. Bluff body with stem and 15 deg semi-angle cone ($M = 1{\cdot}6$).

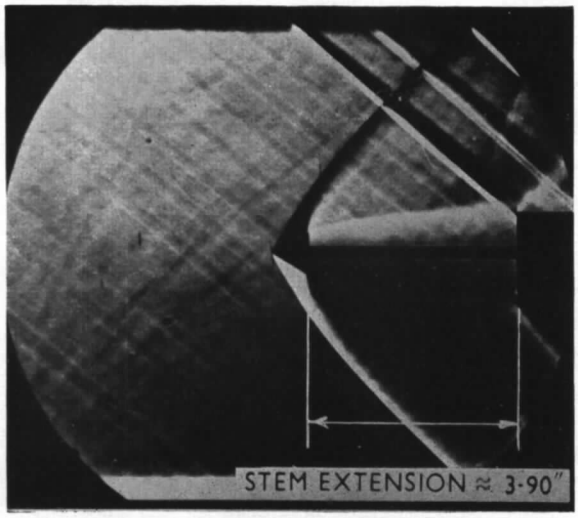


FIG. 19. Bluff body with stem and 30 deg semi-angle cone ($M = 1{\cdot}6$).

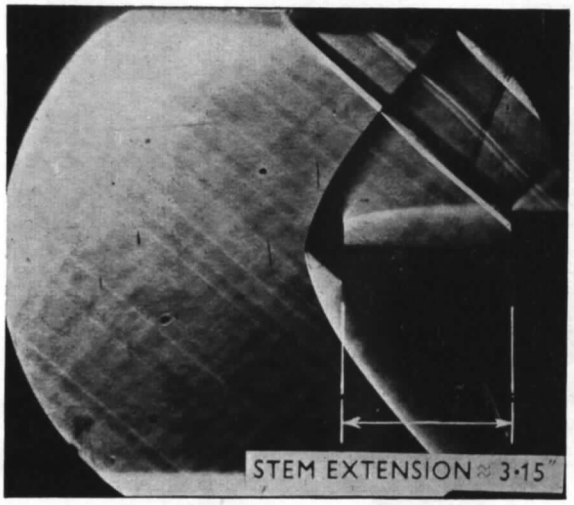


FIG. 20. Bluff body with stem and 40 deg semi-angle cone ($M = 1{\cdot}6$).

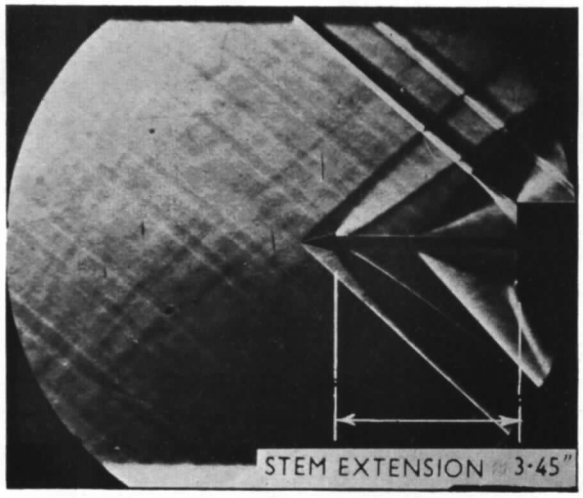


FIG. 21. Bluff body with stem and 15 deg semi-angle cone ($M = 1{\cdot}6$).

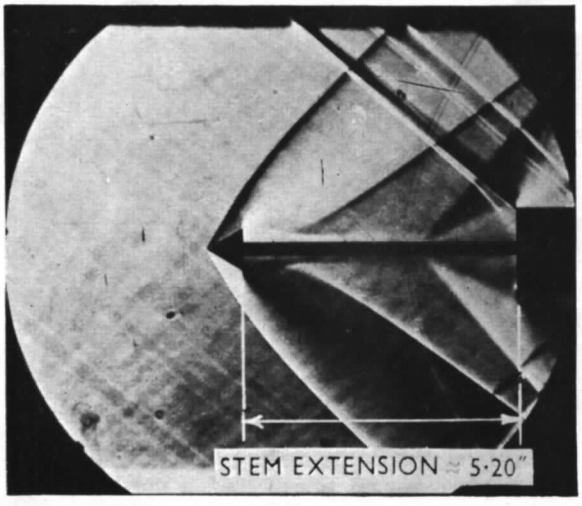


FIG. 22. Bluff body with stem and 30 deg semi-angle cone ($M = 1{\cdot}6$).

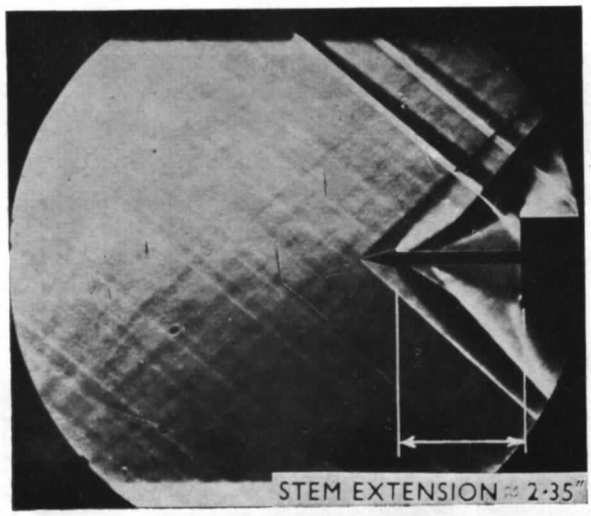


FIG. 23. Bluff body with stem and 15 deg semi-angle cone ($M = 1{\cdot}6$) (stem receding).

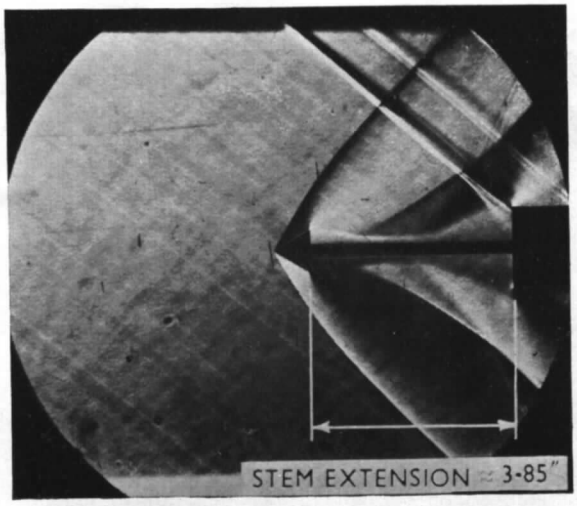


FIG. 24. Bluff body with stem and 30 deg semi-angle cone ($M = 1{\cdot}6$) (stem receding).

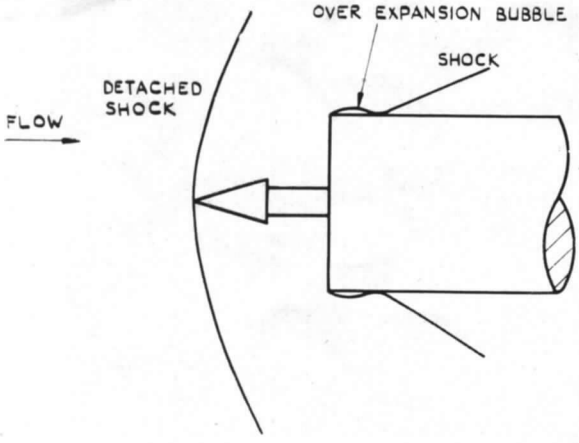


FIG. 25. Flow satisfied by detached shock.

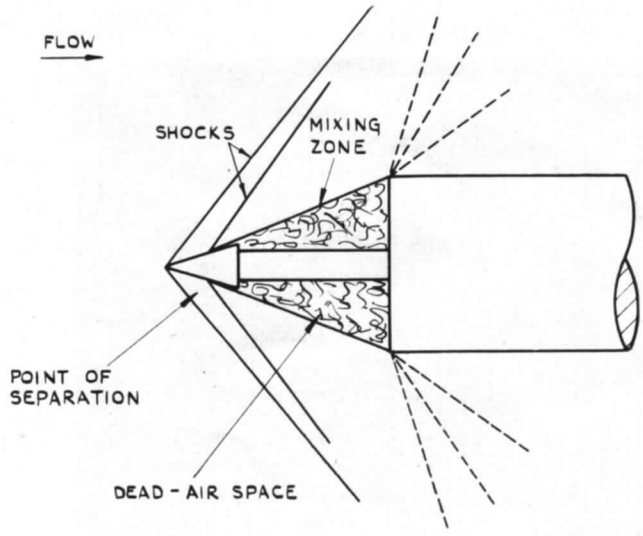


FIG. 26. Flow satisfied by separation from cone.

J4373 Wt.20/9036 K9 10/56 D&Co. 34/263

PRINTED IN GREAT BRITAIN

# Publications of the Aeronautical Research Council

## ANNUAL TECHNICAL REPORTS OF THE AERONAUTICAL RESEARCH COUNCIL (BOUND VOLUMES)

1939 Vol. I. Aerodynamics General, Performance, Airscrews, Engines. 50*s*. (51*s*. 9*d*.)
Vol. II. Stability and Control, Flutter and Vibration, Instruments, Structures, Seaplanes, etc. 63*s*. (64*s*. 9*d*.)

1940 Aero and Hydrodynamics, Aerofoils, Airscrews, Engines, Flutter, Icing, Stability and Control, Structures, and a miscellaneous section. 50*s*. (51*s*. 9*d*.)

1941 Aero and Hydrodynamics, Aerofoils, Airscrews, Engines, Flutter, Stability and Control, Structures. 63*s*. (64*s*. 9*d*.)

1942 Vol. I. Aero and Hydrodynamics, Aerofoils, Airscrews, Engines. 75*s*. (76*s*. 9*d*.)
Vol. II. Noise, Parachutes, Stability and Control, Structures, Vibration, Wind Tunnels. 47*s*. 6*d*. (49*s*. 3*d*.)

1943 Vol. I. Aerodynamics, Aerofoils, Airscrews. 80*s*. (81*s*. 9*d*.)
Vol. II. Engines, Flutter, Materials, Parachutes, Performance, Stability and Control, Structures. 90*s*. (92*s*. 6*d*.)

1944 Vol. I. Aero and Hydrodynamics, Aerofoils, Aircraft, Airscrews, Controls. 84*s*. (86*s*. 3*d*.)
Vol. II. Flutter and Vibration, Materials, Miscellaneous, Navigation, Parachutes, Performance, Plates and Panels, Stability, Structures, Test Equipment, Wind Tunnels. 84*s*. (86*s*. 3*d*.)

1945 Vol. I. Aero and Hydrodynamics, Aerofoils. 130*s*. (132*s*. 6*d*.)
Vol. II. Aircraft, Airscrews, Controls. 130*s*. (132*s*. 6*d*.)
Vol. III. Flutter and Vibration, Instruments, Miscellaneous, Parachutes, Plates and Panels, Propulsion. 130*s* (132*s*. 3*d*.)
Vol. IV. Stability, Structures, Wind tunnels, Wind Tunnel Technique. 130*s*. (132*s*. 3*d*.)

## ANNUAL REPORTS OF THE AERONAUTICAL RESEARCH COUNCIL—

1937 2*s*. (2*s*. 2*d*.) 1938 1*s*. 6*d*. (1*s*. 8*d*.) 1939–48 3*s*. (3*s*. 3*d*.)

## INDEX TO ALL REPORTS AND MEMORANDA PUBLISHED IN THE ANNUAL TECHNICAL REPORTS, AND SEPARATELY—

April, 1950 – – – – – R. & M. No. 2600. 2*s*. 6*d*. (2*s*. 8*d*.)

## AUTHOR INDEX TO ALL REPORTS AND MEMORANDA OF THE AERONAUTICAL RESEARCH COUNCIL—

1909–January, 1954 – – – R. & M. No. 2570. 15*s*. (15*s*. 6*d*.)

## INDEXES TO THE TECHNICAL REPORTS OF THE AERONAUTICAL RESEARCH COUNCIL—

| | | |
|---|---|---|
| December 1, 1936 — June 30, 1939. | R. & M. No. 1850. | 1*s*. 3*d*. (1*s*. 5*d*.) |
| July 1, 1939 — June 30, 1945. – | R. & M. No. 1950. | 1*s*. (1*s*. 2*d*.) |
| July 1, 1945 — June 30, 1946. – | R. & M. No. 2050. | 1*s*. (1*s*. 2*d*.) |
| July 1, 1946 — December 31, 1946. | R. & M. No. 2150. | 1*s*. 3*d*. (1*s*. 5*d*.) |
| January 1, 1947 — June 30, 1947. – | R. & M. No. 2250. | 1*s*. 3*d*. (1*s*. 5*d*.) |

## PUBLISHED REPORTS AND MEMORANDA OF THE AERONAUTICAL RESEARCH COUNCIL—

| | | |
|---|---|---|
| Between Nos. 2251–2349. – – | R. & M. No. 2350. | 1*s*. 9*d*. (1*s*. 11*d*.) |
| Between Nos. 2351–2449. – – | R. & M. No. 2450. | 2*s*. (2*s*. 2*d*.) |
| Between Nos. 2451–2549. – – | R. & M. No. 2550. | 2*s*. 6*d*. (2*s*. 8*d*.) |
| Between Nos. 2551–2649. – – | R. & M. No. 2650. | 2*s*. 6*d*. (2*s*. 8*d*.) |

*Prices in brackets include postage*

HER MAJESTY'S STATIONERY OFFICE

York House, Kingsway, London W.C.2; 423 Oxford Street, London W.1;
13a Castle Street, Edinburgh 2; 39 King Street, Manchester 2; 2 Edmund Street, Birmingham 3; 109 St. Mary Street, Cardiff; Tower Lane, Bristol 1; 80 Chichester Street, Belfast, *or through any bookseller*

S.O. Code No. 23-3007